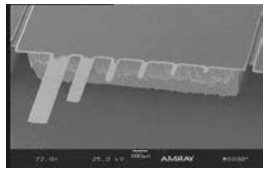
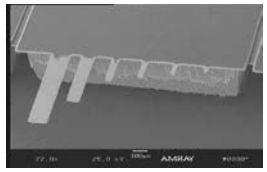
# About OMICS Group



OMICS Group International is an amalgamation of Open Access publications and worldwide international science conferences and events. Established in the year 2007 with the sole aim of making the information on Sciences and technology 'Open Access', OMICS Group publishes 400 online open access scholarly journals in all aspects of Science, Engineering, Management and Technology journals. OMICS Group has been instrumental in taking the knowledge on Science & technology to the doorsteps of ordinary men and women. Research Scholars, Students, Libraries, Educational Institutions, Research centers and the industry are main stakeholders that benefitted greatly from this knowledge dissemination. OMICS Group also organizes 300 International conferences annually across the globe, where knowledge transfer takes place through debates, round table discussions, poster presentations, workshops, symposia and exhibitions.

# About OMICS Group Conferences



OMICS Group International is a pioneer and leading science event organizer, which publishes around 400 open access journals and conducts over 300 Medical, Clinical, Engineering, Life Sciences, Pharma scientific conferences all over the globe annually with the support of more than 1000 scientific associations and 30,000 editorial board members and 3.5 million followers to its credit.

OMICS Group has organized 500 conferences, workshops and national symposiums across the major cities including San Francisco, Las Vegas, San Antonio, Omaha, Orlando, Raleigh, Santa Clara, Chicago, Philadelphia, Baltimore, United Kingdom, Valencia, Dubai, Beijing, Hyderabad, Bengaluru and Mumbai.



# Nanomechanical Biosensors

**Dr. Haifeng (Frank) Ji**

**08/11/2014**

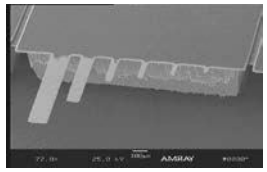
**Associate Professor**

**Department of Chemistry**

**Drexel University**




ANTHONY JOSEPH DREXEL



- J. K. Gimzewski, C. Gerber, E. Meyer, and R. R. Schlittler, "Observation of a Chemical Reaction Using a Micromechanical Sensor," *Chem. Phys. Lett.*, **1994**, *217*, 589-594
- G. Y. Chen, R. J. Warmack, T. Thundat, D. P. Allison, and A. Huang, "Resonance Response of Scanning Force Microscopy Cantilevers," *Rev. Sci. Instrum.* **1994**, *65*, 2532-2537
- T. Thundat, R. J. Warmack, G. Y. Chen, and D. P. Allison "Thermal and ambient-induced deflections of scanning force microscope cantilevers", Appl. Phys. Lett. **1994**, *64*(21), 2894-2896

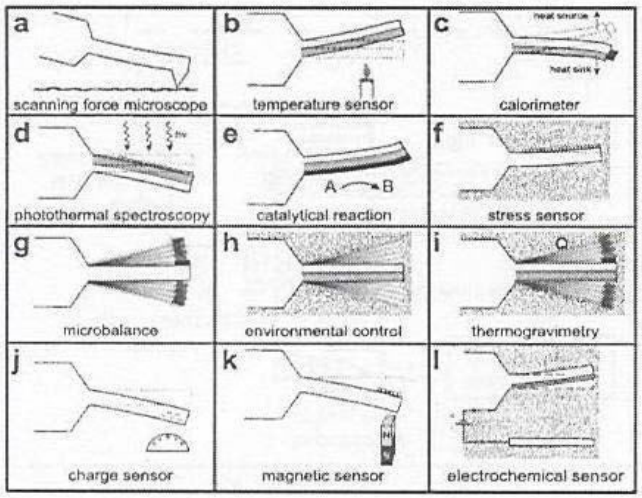
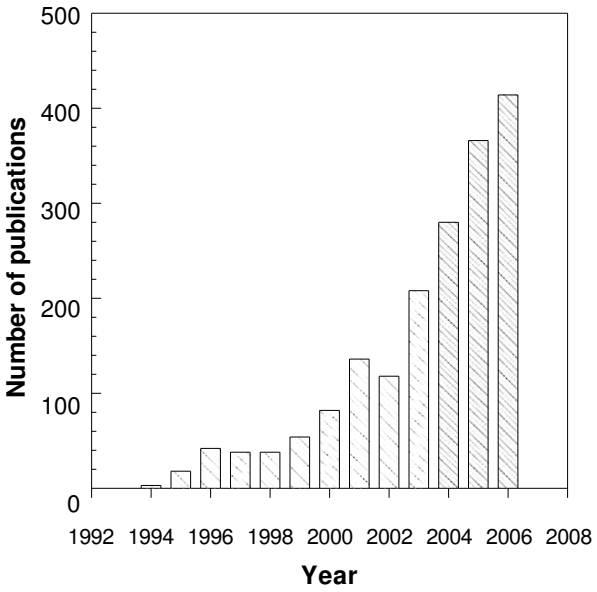
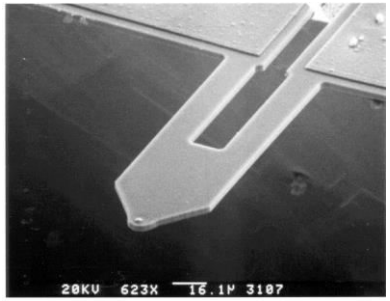



Fig. 1. Operation principles of cantilever-based sensors.





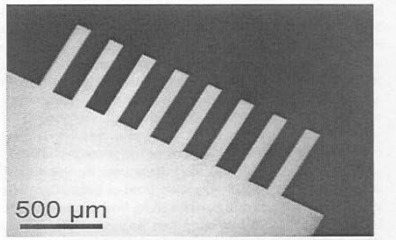
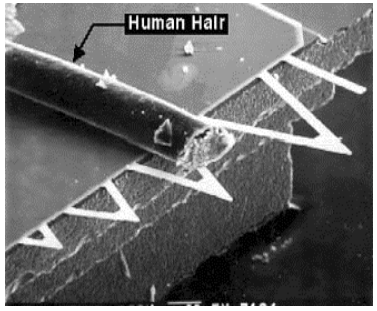
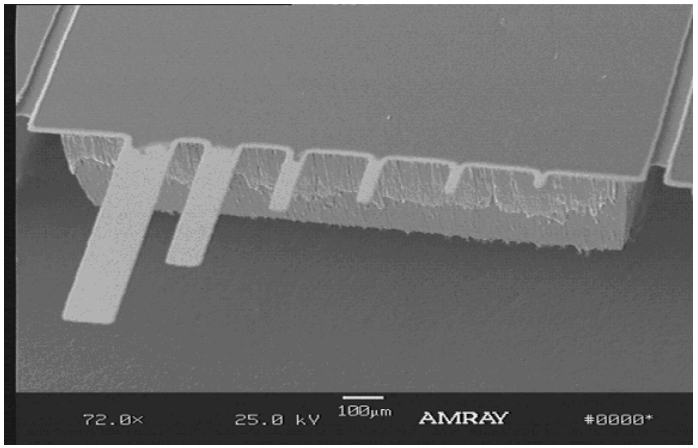
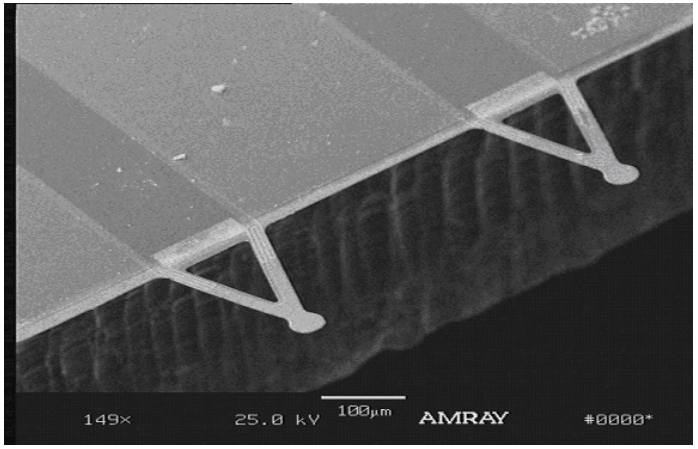
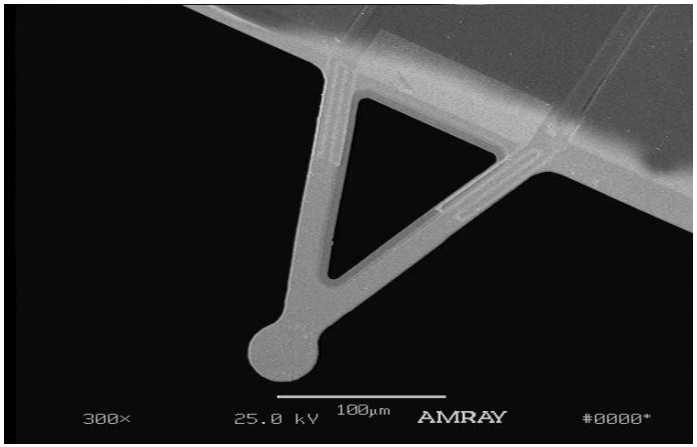




Fig. 2. Optical micrograph of a microfabricated cantilever sensor array produced from silicon in the Micromechanics Department at the IBM Zurich Research Laboratory. Cantilever length: 500 µm, cantilever thickness: 0.8 µm, cantilever width: 100 µm. Typical spring constant: 0.02 N $m^{-1}$.

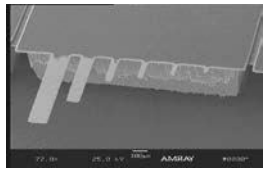



**V-shaped microcantilevers**
**L—200 µm**
**W—40 µm**
**t—2 µm**

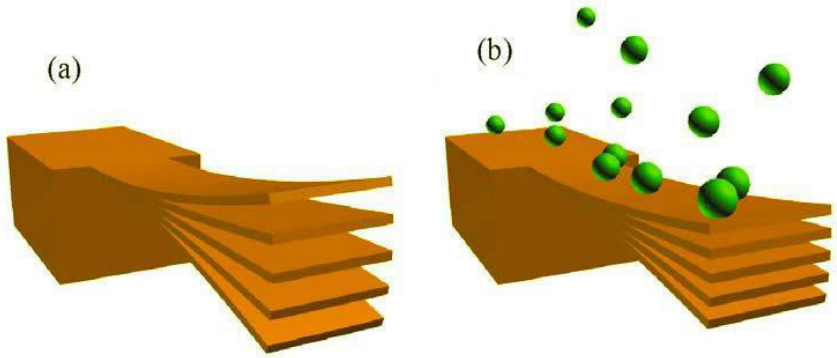


Two independent properties (bending, frequency) of a microcantilever can be simultaneously detected.

Resonance frequency. The resonance frequency of an oscillating cantilever can be expressed as

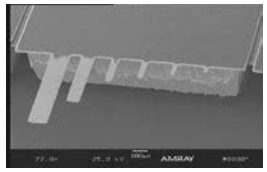
(1)
$$f = \frac{1}{2\pi}\sqrt{\frac{K}{m^*}}$$

where K is the spring constant of the lever and m* is the effective mass of the microcantilever.




Preferred MC: short and stiff ($Si_3N_4$, SiC)

Application: gas



2. Microcantilever bending. One unique characteristics of microcantilevers is that the device can be made to undergo bending due to molecular adsorption by confining the adsorption to one side of the cantilever. Using Stoney's formula, the radius of curvature of bending of the cantilever due to adsorption can be written as:

$$\frac{1}{R} = \frac{6(1-\upsilon)}{Et^2}\delta s \qquad \Delta z = \left(\frac{3(1-\upsilon)L^2}{Et^2}\right)\delta s$$

where R is the radius of curvature for the cantilever, v and E are Poisson's ratio and Young's modulus for the substrate, respectively, ***t*** is the thickness of the cantilever and ds is the film stress.

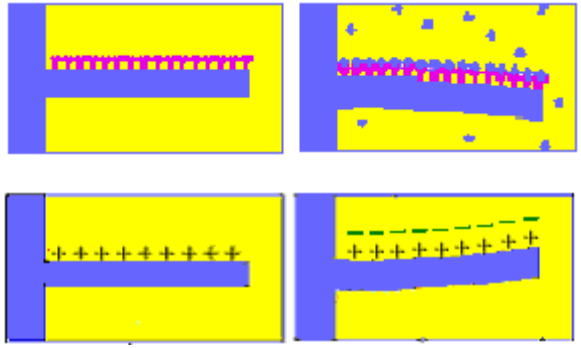
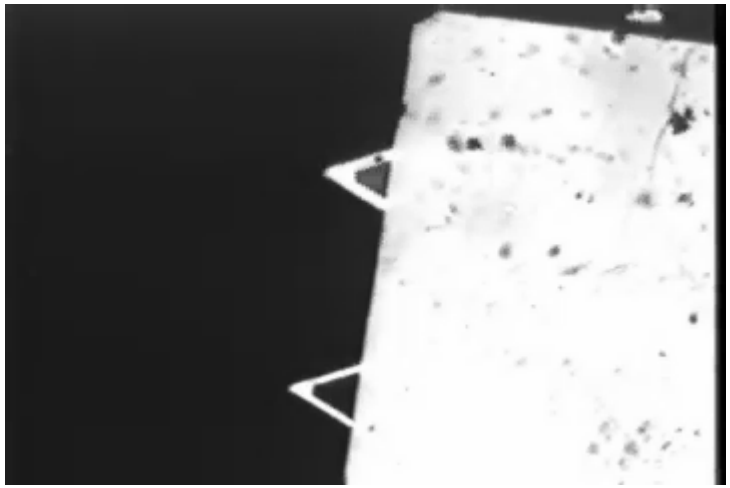
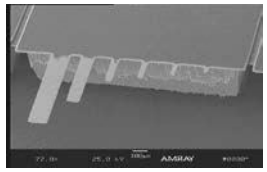


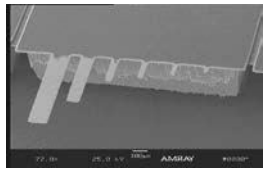
**Figure.** Two mechanisms of binding-induced surface stress in different types of responsive coatings. (Left) Expansive stresses for antigen-antibody interaction (Right) Compressive stress due to neutralization of excessive charge on the surface

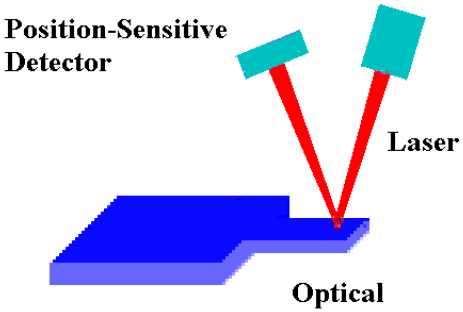


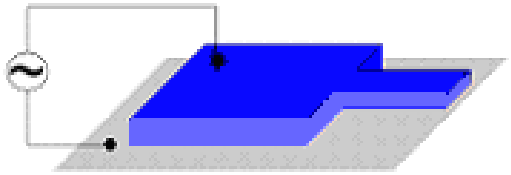
**A modified microcantilever (top) bended down upon exposure to methanol vapor and returned to its original position when the methanol vapor was replaced with air. For comparison, unmodified microcantilever (bottom) did not bend upon exposure to methanol.**



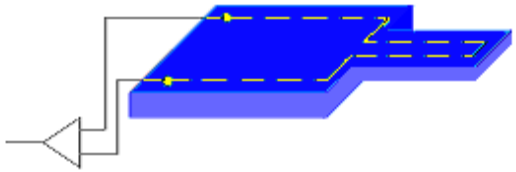
- 1. Piezoelectric sensors -- QCM
- 2. Optical sensors – Fiber optical, Color, FI, Surface plasmon resonance (SPR), Evanescent wave (EW), Laser
- 3. Electrochemical sensors
  - Potentiometric sensors
  - Amperometric sensors
  - Others
- 4. Thermometric sensors, calorimeter
- 5. FET sensors
- 6. Flow meter sensor (nanoporous, microfluidic)
- 7. Cantilever sensors



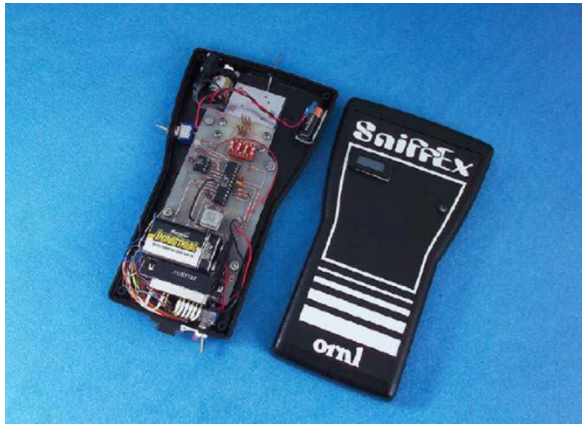


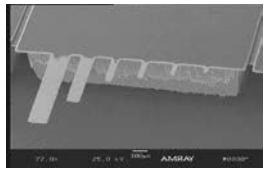
Capacitive



Piezoresistive or
Piezoelectric

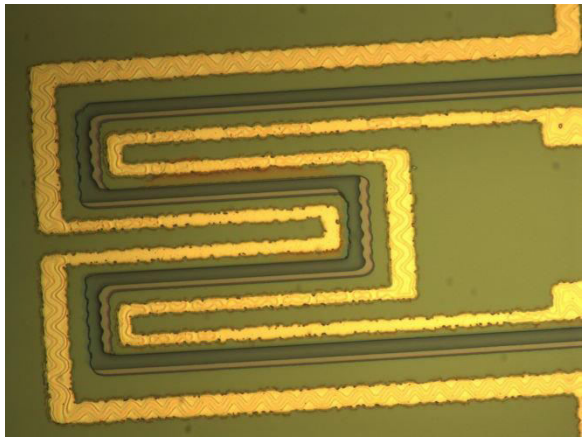



ORNL, Berkeley, GA Tech, Purdue Univ., IBM Switzerland



- Scan tunneling – Univ. Minnesota Nanofabrication Center
- Interferometry – IBM Switzerland
- Electric field gradient distribution – NIST
- Force-Distance – IBM Switzerland
- MOSFET methods – Northwestern Univ. International Institute for Nanotechnology
- Liquid inside the microcantilever – MIT

- The 2008 Conferee Networking (CN) "Micromechanical Chem/Bio Sensors”



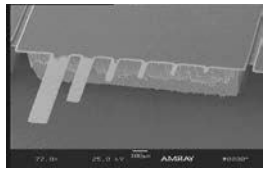
This structure consists of one primary metal coil on a microcantilever and a secondary coil on the surrounding substrate. When voltage is applied on the primary coil, the created magnetic field causes induced voltage on the secondary coil.

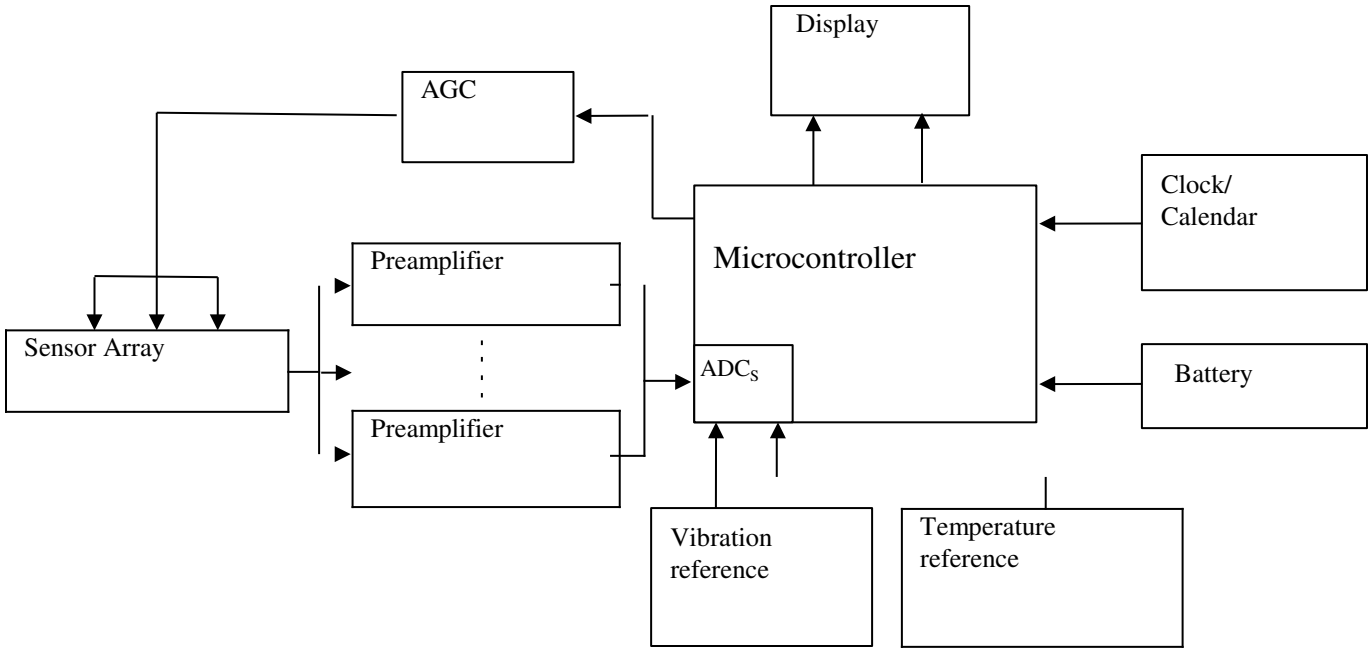
| | $V_{out}$ before bending | **$V'_{out}$ after 100 nm bending** | $\Delta V_{out}$ | **$\Delta V_{out}/V_{out}$** |
|---|---|---|---|---|
| Calculation | 2.8911 | 2.8875 | 0.0036 | **0.125%** |
| Simulation | 2.64279628 | 2.63906121 | 0.00373507 | **0.14133%** |
| Experiment | 2.4723 | 2.4685 | 0.0038 | **0.1537%** |

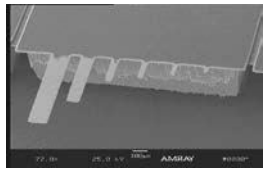
**Table 2**. The Vout of the second coil upon 2 V Vin of the first coil. The two coils are separated by **10** μm. The thickness and width of the coils are 1 mm, and 10 mm, respectively.

| Method | $V_{out}$ (mV) (before bending) | **$V_{out}$ (mV) (with 1 nm bending)** | **$\Delta V/V_{out}$** |
|---|---|---|---|
| Calculation | 279.89 | 279.24 | **0.23%** |
| Simulation | 256.3556735 | 255.7546534 | **0.24%** |

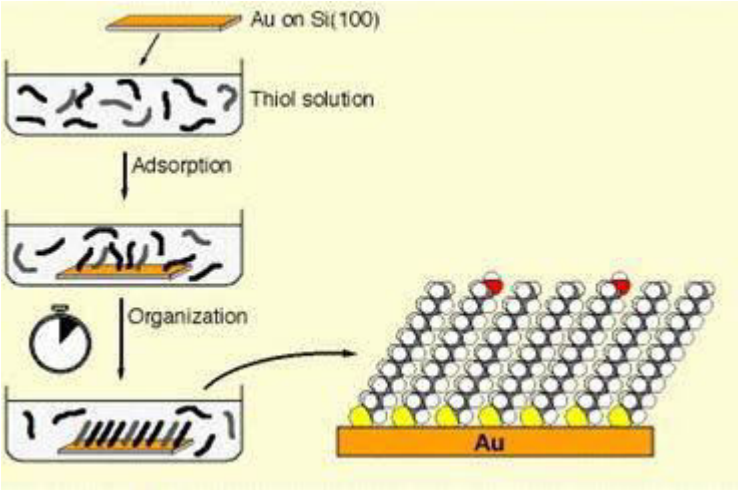
**Table 3**. The Vout of the second coil upon 2 V Vin of the first coil. The two coils are separated by **1** μm. The thickness and width of the coils are 1 mm, and 10 mm, respectively.



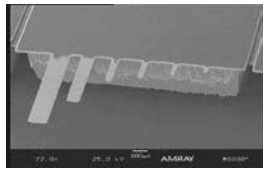

Display
AGC
Clock/
Calendar
Microcontroller
Preamplifier
Sensor Array
ADCs
Battery
Preamplifier
Vibration
reference
Temperature
reference



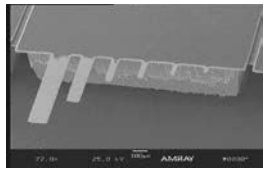
# 1. Self Assembled Monolayers and Surface Conjugation Chemistry



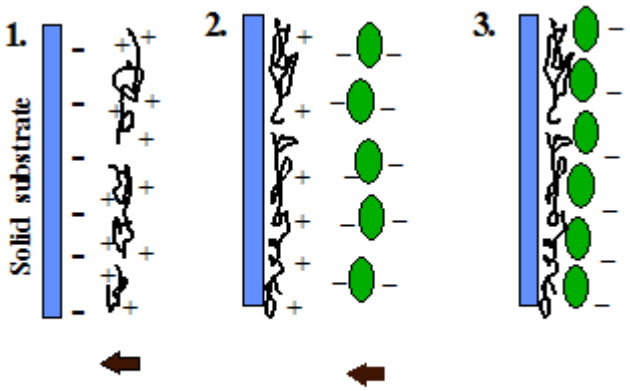

Chemical modification of the silica and gold surface is well developed. Some of the common choices include:
(A) Carboxyl (-COOH)-modified cantilever,
(B) Amino (-NH2)-modified cantilever,
(C) Hydroxyl (-OH)-modified cantilever,
(D) Hydrazide (-NHNH2)-modified cantilever,
(E) Amide (-CONH2)-modified cantilever;
(F) Chloromethyl (-CH2Cl)-modified cantilever,
(G) Epoxy-modified cantilever,
(H) Aldehyde (-CHO)-modified cantilever
(I) Tosyl-modified cantilever.

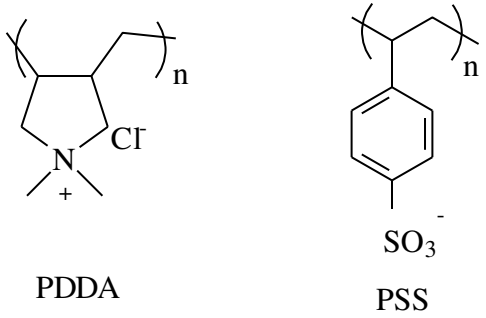


| Receptors | Analytes | D amplitudes | Mechanism | Comments |
|---|---|---|---|---|
| 18-crown-6 | $K^+$ | 0 nm | Crown ether-ions | |
| 15-crown-5 | $Na^+$ | 0 nm | Crown ether-ions | |
| calixcrown | $Sr^{2+}$ | 0 nm | Calix-crown-ions | |
| Glucose oxidase | glucose | 7 nm | Enzyme-organic | Depend on |
| AChE | OPs | 9 nm | Enzyme-organic | Conjugation |
| Cystein-$Cu^{2+}$ complex | OPs | 30 nm | Complex-organic | Chemistry |
| SH group | $HgMe^+$ | 22 nm | Complex-ions | |
| phosphate | $Ca^{2+}$ | 40 nm | Ion pairs | |
| Anti-Cd-EDTA | EDTA-$Cd^{2+}$ | 100 nm | Antibody-ions | |
| cysteine | $Cu^{2+}$ | 150 nm | Ion pairs | |
| ammonium | $CrO_4^{2-}$ | 450 nm | Ion pair | |
| Anti-SARS | SARS | 800 nm | Antibody-Bacteria | |
| Anti-E.Coli | E. Coli | 800 nm | Antibody-Bacteria | |
| Anti-Tularemia | Tularemia | 700 nm | Antibody-Virus | |
| | | | | |

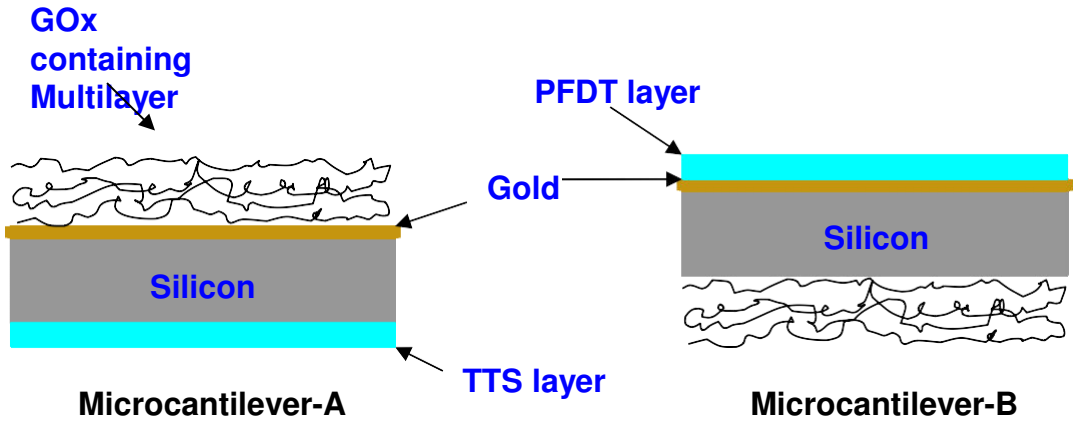


## 2. Self Assembled Multilayers

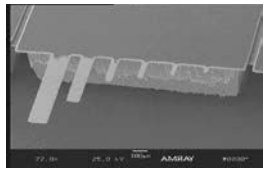


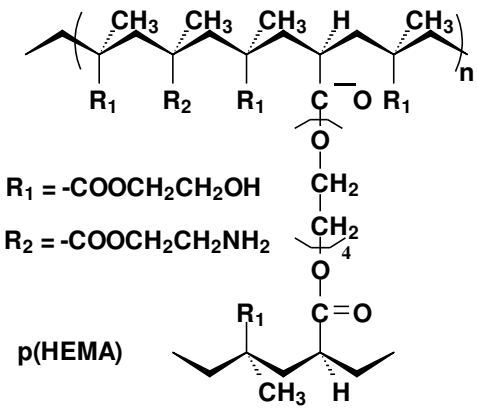

PDDA PSS

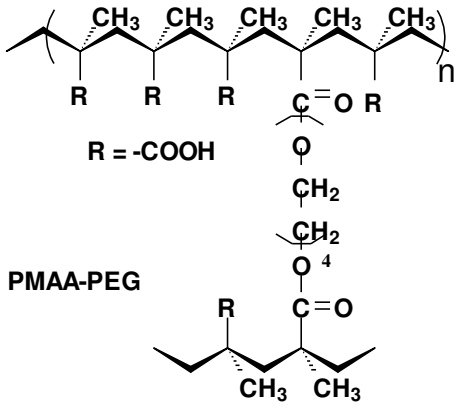


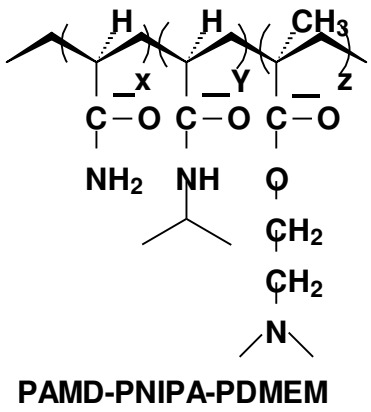

The example of PDDA/PSS modification process of a microcantilever

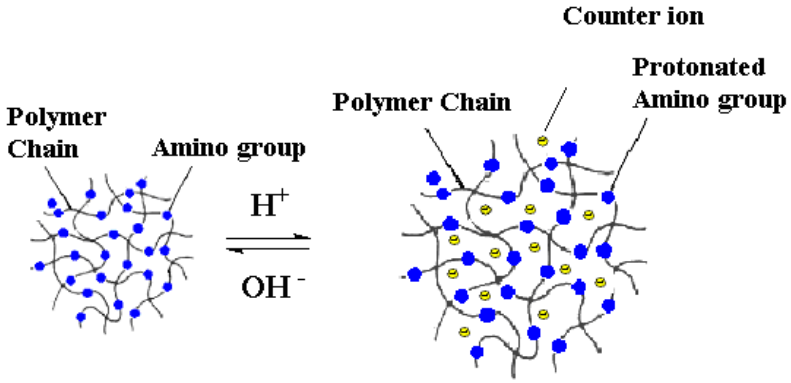


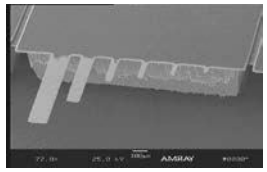
# Structures of several pH sensitive hydrogels



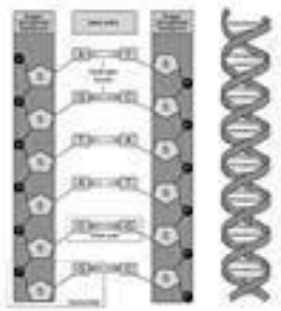



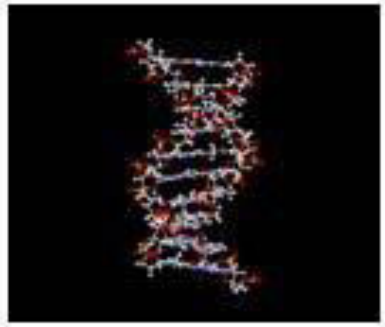



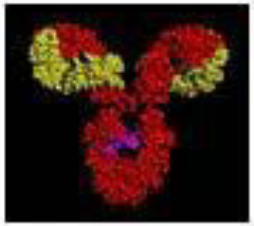



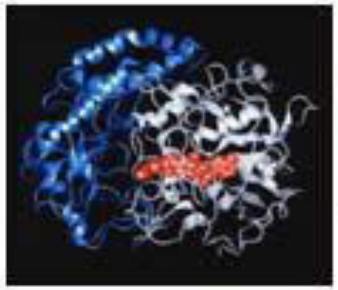


- **Biosensors**
  - Biosensor 1: DNA hybridization on the cantilever surface
  - **Biosensor 2. Antibody based sensors, examples: E. Coli, Tularemia, and SARS**
  - Biosensor 3. Membrane based sensors, example, serotonin for drug screening
  - **Biosensor 4: Enzyme based sensors, example, glucose, OPs**
  - **Biosensor 5. Other proteins based sensors, such as for $Ca^{2+}$.**
  - **Whole cell**
  - Whole organs/systems

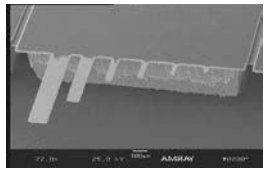






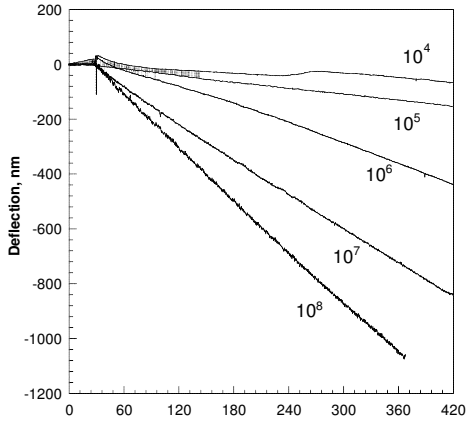






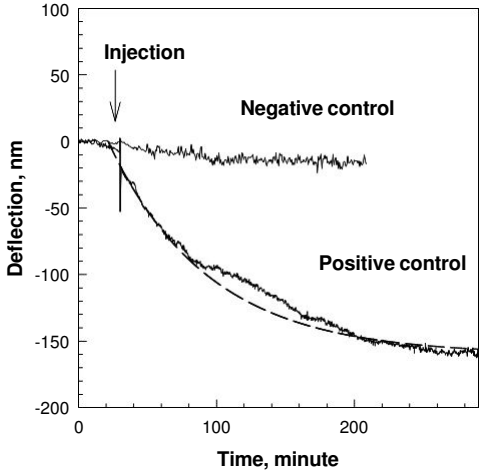
*Tularemia (Francisella tularensis)* is a small, nonmotile, aerobic, gram-negative coccobacillus. It is one of the most infectious pathogenic bacteria known.

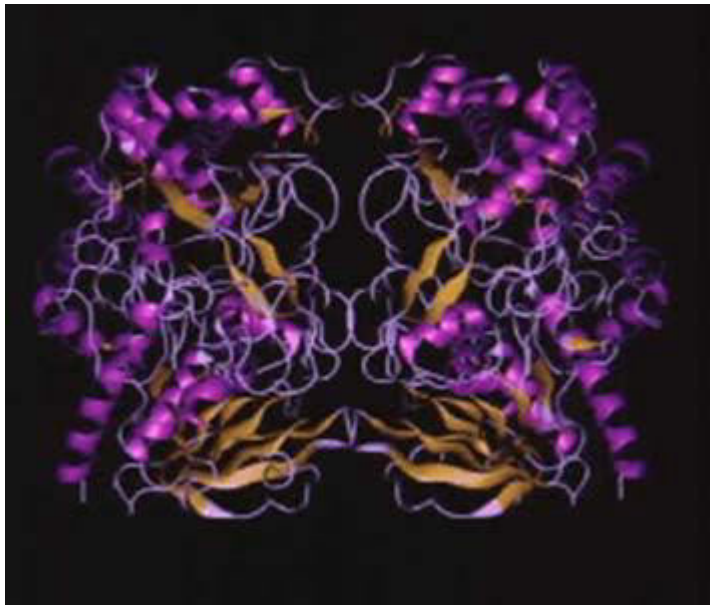
Bending response as a function of time for antibody immobilized microcantilevers upon injection of different concentration (organisms/mL) solutions of F. Tularensis in 0.1M phosphate-buffered saline buffer (pH=7.3)




E. coli O157:H7, first recognized in 1982 in the United States, is an epidemiologically significant cause of food borne disease worldwide. E. coli O157:H7 can readily contaminate ground beef, raw milk, poultry products, fresh apple cider, cold sandwiches, vegetables, and drinking water supplies.

Bending response as a function of time for an antibody immobilized microcantilever upon injection of a $5\times10^6$ cfu/mL solution of E.coli O157:H7 in 0.1M PBS buffer (pH=7.3)

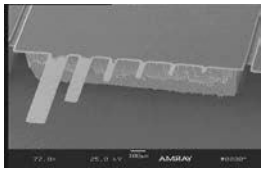


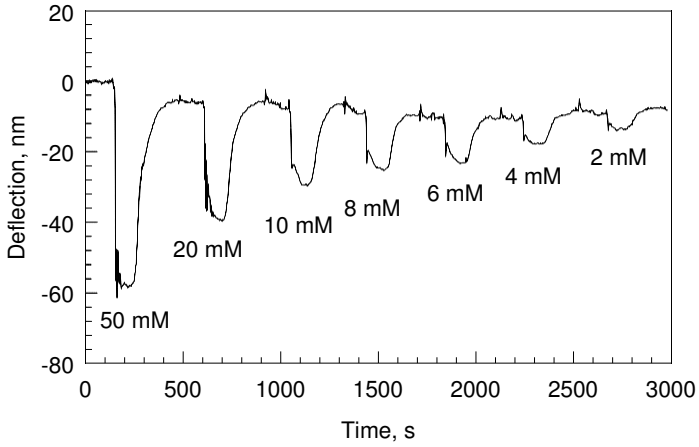


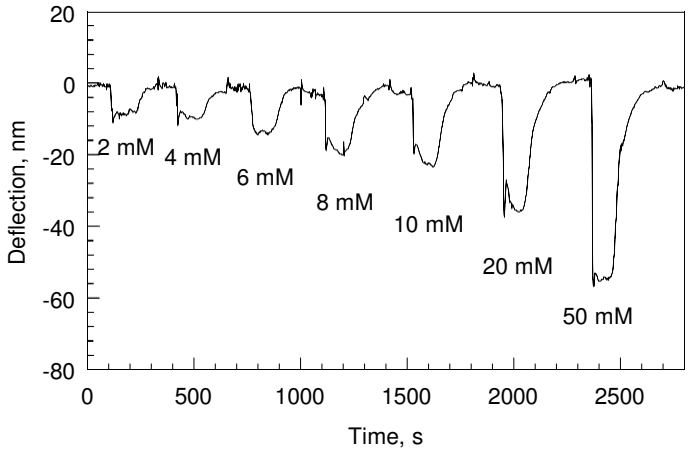
Supported by US Army-Technologies for Metabolic Monitoring

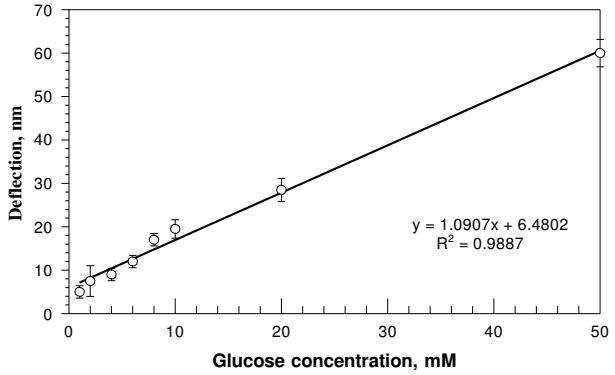
**topology of Glucose Oxidase (GOx) enzyme**

$$\beta - D - glu\cos e + O_2 + H_2O \xrightarrow{Glucose\ Oxidase} D - gluconic\ acid + H_2O_2$$

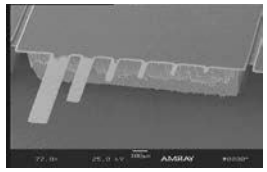


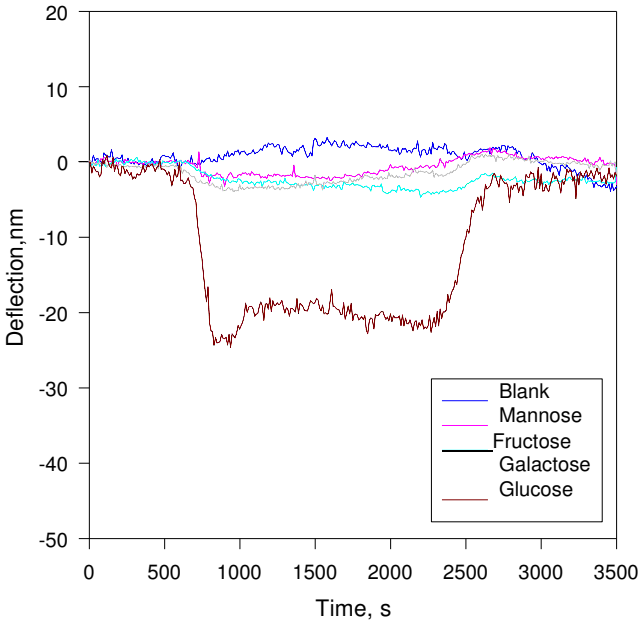


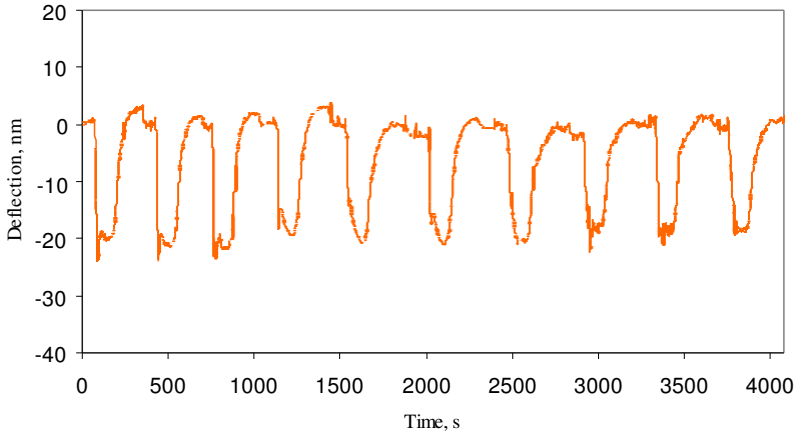



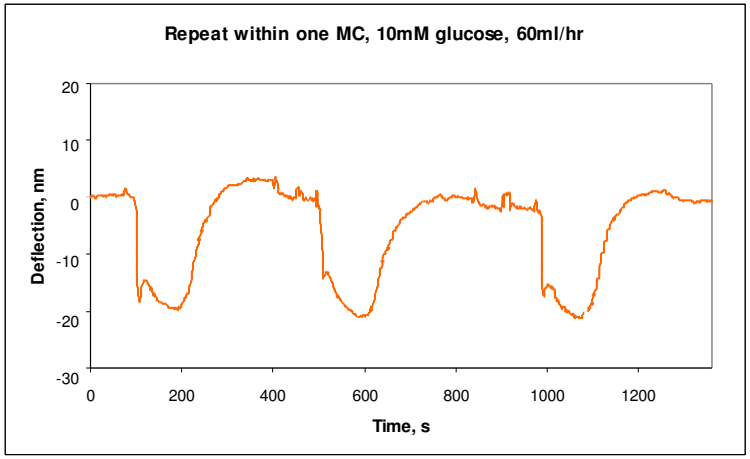




**Deflection of microcantilever modified by glucose oxidase multilayer vs. the concentration of different glucose solutions.**

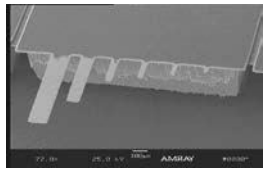





MCL deflection with exposure to glucose, mannose, fructose, and galactose at concentration of 10 mM.



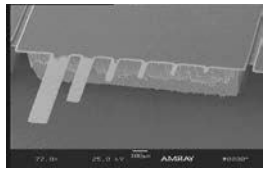
$$\beta - D - Glu\cos e \xrightarrow{GOx} GluconicAcid + H_2O_2 \text{ - 80 kcal/mol}$$

$$E_{ox} + G \xrightarrow{k_1} GOx - G$$

$$GOx - G \xrightarrow{K_2} gluconicacid + E_{red}$$

$$E_{red} + O_2 \xrightarrow{K_3} E_{ox} + H_2O_2$$

$$V = \frac{C_E k_2}{1 + \frac{k_2}{k_1[G]} + \frac{k_2}{k_3[O_2]}}$$



$$\beta - D - Glu\cos e \xrightarrow{GOx} GluconicAcid + H_2O_2 \qquad -80\ KJ/mol$$

The conversion rate of glucose in the thin multilayer film calculated above is corresponding to 8.85 x $10^{-12}$ mol / min, and it would produce thermal output (dQ/dt) on the order of 7.2 x$10^{-9}$ J/s. At equilibrium or steady state, the temperature difference between the GOx/PEI multilayer covered surface and the surroundings is constant, i.e. the dT/dt = 0. From one-dimensional heat flow equation, the heat flow can be given by:

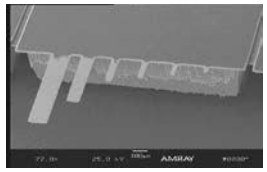
$$\frac{dQ}{dt} = kA\left(\frac{dT}{dx}\right)_{x\to o^-} + hA\left(\frac{dT}{dx}\right)_{x-o^+}$$

where k is the thermal conductivity of silicon (83.5 W/m K), A is the MCL surface area (8.51x$10^{-3}$ $mm^2$), h is the convection coefficient of water in these experimental conditions (1020 W/$m^2$•K) that can be calculated from Nux, assuming the water is laminar flow (see supplemental materials).
Thus, solving the equation 9 revealed that the temperature difference between the GOx/gold surface and surrounding solutions (DT) was 7.7x$10^{-4}$ K.

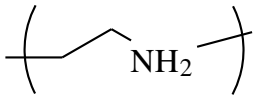
$$\Delta T = \frac{h[3(1+m)^2 + (1+mn)(m^2 + \frac{1}{mn})}{6(\alpha_1 - \alpha_2)(1+m)^2} \frac{2D}{L^2 + D^2}$$

Calculation results show that thermal effect can cause only 7x$10^{-3}$ nm deflection.

**Contribution from thermal change is negligible.**



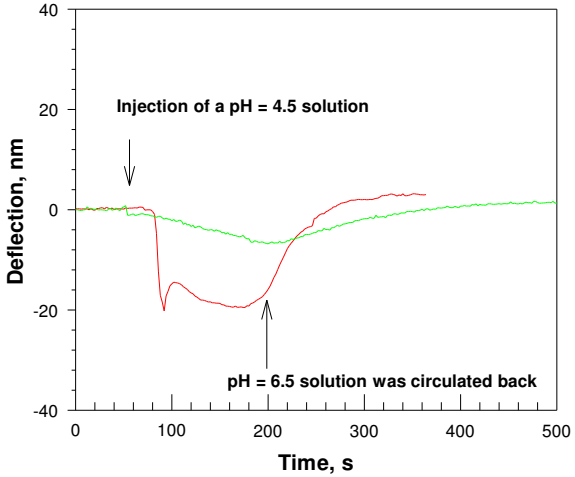
$$\beta - D - Glu\cos e \xrightarrow{GOx} GluconicAcid + H_2O_2$$




**PEI**

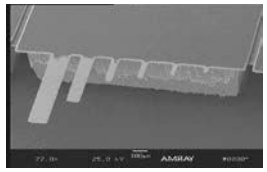
$$\frac{\partial P}{\partial t} = V - D_P \frac{\partial^2 P}{\partial x^2} = \frac{C_E k_2}{1 + \frac{k_2}{k_1[G]} + \frac{k_2}{k_3[O_2]}} - D_P \frac{\partial^2 P}{\partial x^2}$$

$$D_P \frac{\partial^2 P}{\partial x^2} = \frac{C_E k_2}{1 + \frac{k_2}{k_1[G]} + \frac{k_2}{k_3[O_2]}}$$




pH changes from 6.5 to 4.5

**The pH change in the multilayer surface does not contribute significantly to the MCL deflection**



$$Glu\cos e + E_{ox} \rightarrow GluconicAcid + E_{red}$$

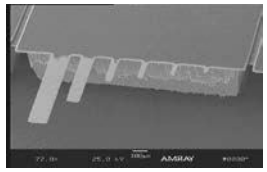
$$E_{red} + O_2 \rightarrow E_{ox} + H_2O_2$$

$$\frac{\partial P}{\partial t} = V - D_P \frac{\partial^2 P}{\partial x^2} = \frac{C_E k_2}{1 + \frac{k_2}{k_1[G]} + \frac{k_2}{k_3[O_2]}} - D_P \frac{\partial^2 P}{\partial x^2} \qquad D_P \frac{\partial^2 P}{\partial x^2} = \frac{C_E k_2}{1 + \frac{k_2}{k_1[G]} + \frac{k_2}{k_3[O_2]}}$$

**At equilibrium, the [$H_2O_2$] = 0.01 mM.**

**Control experiments showed that no bending was observed upon exposure of the MC to a 10 mM $H_2O_2$ solution.**

**Hydrogen peroxide has no contribution to the deflection of microcantilever.**



$$\beta - D - Glu\cos e \xrightarrow{GOx} GluconicAcid + H_2O_2 + 80\ \text{kJ/mol}$$

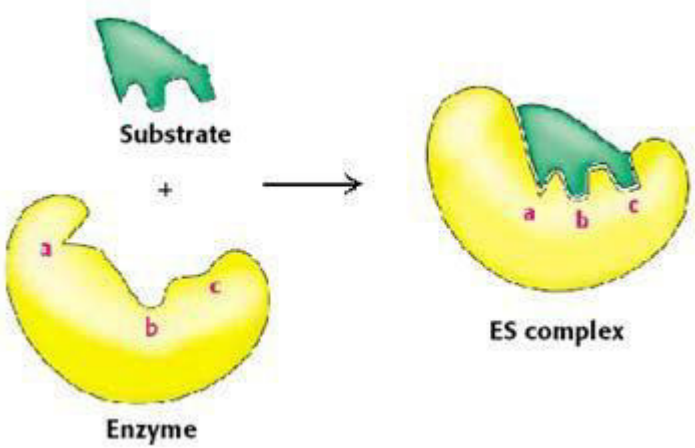
$$E_{ox} + G \xrightarrow{k_1} GOx - G$$

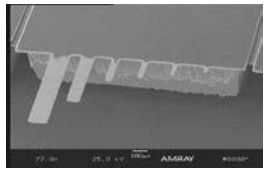
$$GOx - G \xrightarrow{k_2} gluconicacid + E_{red}$$

$$E_{red} + O_2 \xrightarrow{k_3} E_{ox} + H_2O_2$$

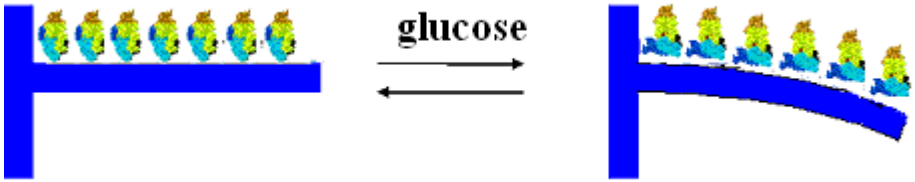
$$V = \frac{C_E k_2}{1 + \frac{k_2}{k_1[G]} + \frac{k_2}{k_3[O_2]}}$$

Induced fit: binding good substrate causes enzyme to fold to active conformation

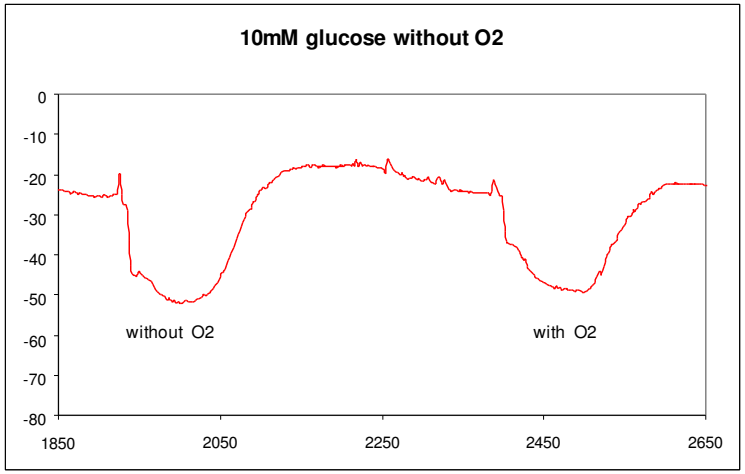




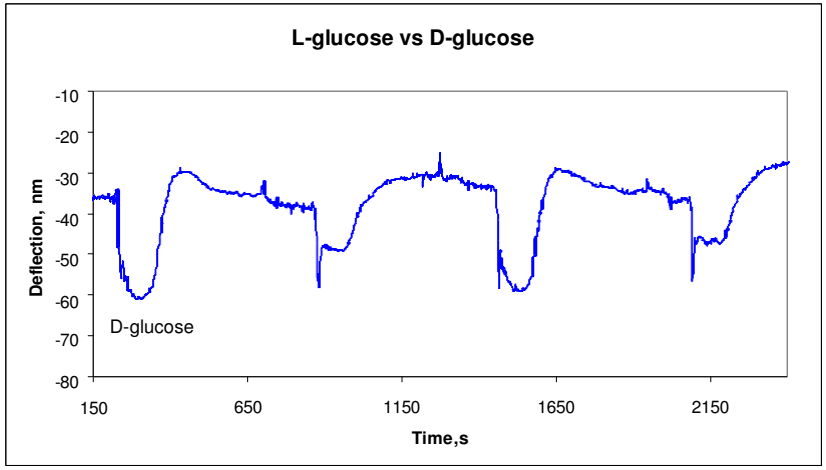
$$E_{OX} + Glu\cos e \rightarrow E_{RED} \bullet Glu\cos e$$
$$E_{RED} \bullet Glu\cos e \rightarrow E_{RED} + GluconicAcid$$
$$E_{RED} + O_2 \rightarrow E_{OX} \bullet H_2O_2$$
$$E_{OX} \bullet H_2O_2 \rightarrow E_{OX} + H_2O_2$$



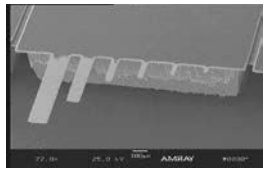

## Evidence 1




## Evidence 2

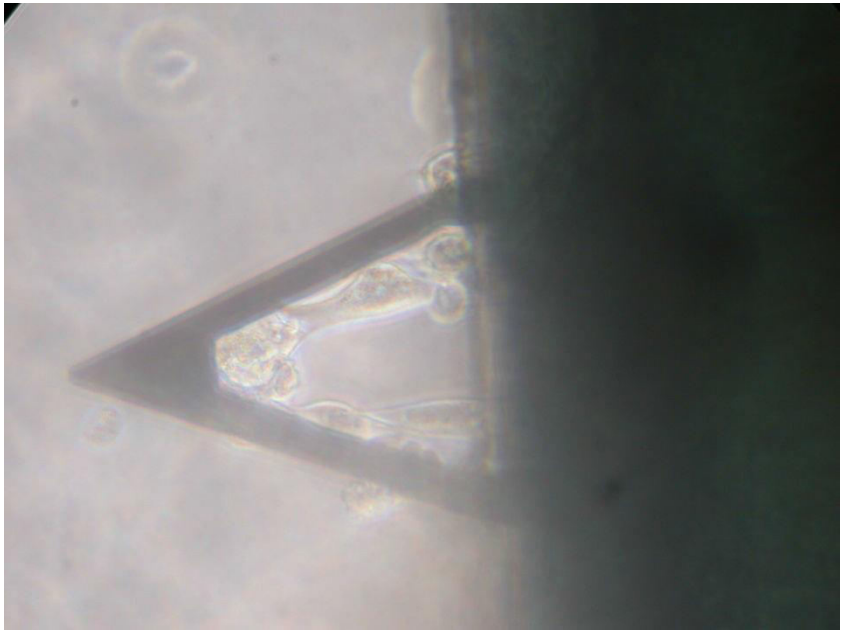



**Conclusion: GOx conformational change Is most likely the primary source for MCL deflection**

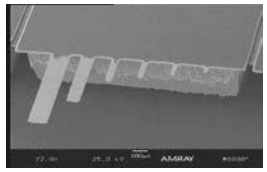


- Conformational change of the proteins is most likely the primary source of the nanomechanical bending.
  - The MCL technique offers unique opportunities in the design of small and cost-effective analytical methods for studying the conformational change of proteins and protein-ligand interaction under varying conditions of ionic strength or electrolyte identity. Advantages are reduces costs and fast throughput characteristics. (NIH SBIR/STTR)
  - It provides an alternative, label-free bioassay for drug screening applications. (NIH R01)

- Biomolecular design to enhance the $k_1$ of the enzyme-analyte binding could be another approach to increase the sensitivity. (traditionally, increasing reaction rate was used to increase the sensitivity).
  - OPH variants modified MCLs may provide a highly **sensitive** device in nerve agents **monitoring**. (NSF/DOD/EPA)



# *Let Us Meet Again*



We welcome you all to our future conferences of OMICS Group International

Please Visit:

www.omicsgroup.com

www.conferenceseries.com

www.pharmaceuticalconferences.com